

Structure-Function Approach to Vector-Boson Scattering in pp Collisions

T. Han, G. Valencia, and S. Willenbrock*

Fermi National Accelerator Laboratory

P.O. Box 500, Batavia, IL 60510

Abstract

We discuss weak-vector-boson scattering, at next-to-leading order in QCD, within the framework of hadronic structure functions. We use this approach to calculate the Higgs-boson production cross section via vector-boson fusion at the LHC/SSC; we find a modest increase over the leading-order prediction. We also give expressions for the distribution of vector bosons in a proton (effective- W approximation) including $\mathcal{O}(\alpha_s)$ corrections.

[*]Permanent address: Physics Department, Brookhaven National Laboratory, Upton, NY 11973



The LHC/SSC will be the first machines capable of studying weak-vector-boson scattering, where the "initial" vector bosons are radiated from the quarks and anti-quarks which reside in the proton. It is believed that this process will yield clues to the mechanism which breaks the electroweak symmetry [1], which is one of the outstanding puzzles of high-energy physics. For example, in the standard Higgs model of electroweak-symmetry breaking, the Higgs boson is copiously produced via vector-boson fusion [2, 3].

In this paper we show that weak-vector-boson scattering may be calculated in terms of the charged-current and neutral-current hadronic structure functions $F_i(x, Q^2)$ ($i = 1, 2, 3$). One advantage of this approach is that the $\mathcal{O}(\alpha_s)$ QCD correction to vector-boson scattering can be incorporated simply by employing the QCD-corrected expressions for the structure functions in the parton model. This constitutes a considerable simplification of the calculation. The resulting cross section is differential in the vector-boson scattering subprocess. A similar approach has been applied to two-photon processes [4].

As usual, we write the hadronic tensor $W_{\mu\nu}$ in terms of the three structure functions:

$$\begin{aligned}
 MW_{\mu\nu}(x, Q^2) &= F_1(x, Q^2) \left(-g_{\mu\nu} + \frac{q_\mu q_\nu}{q^2} \right) \\
 &+ \frac{F_2(x, Q^2)}{P \cdot q} \left(P_\mu - \frac{P \cdot q}{q^2} q_\mu \right) \left(P_\nu - \frac{P \cdot q}{q^2} q_\nu \right) \\
 &- i \frac{F_3(x, Q^2)}{2P \cdot q} \epsilon_{\mu\nu\rho\sigma} P^\rho q^\sigma
 \end{aligned} \tag{1}$$

where M is the proton mass, P_μ is the proton four-momentum, q_μ is the vector-boson four-momentum, $Q^2 = -q^2$, and $x = Q^2/2P \cdot q$. Vector-boson scattering in pp collisions is then calculated by contracting the hadronic tensors at each vertex with

the tensor corresponding to the square of the vector-boson-scattering subprocess, as in Fig. 1. We find

$$d\sigma = \frac{1}{2S} 4 \frac{g_{V_1}^2}{8} \frac{g_{V_2}^2}{8} \frac{1}{(Q_1^2 + M_{V_1}^2)^2} \frac{1}{(Q_2^2 + M_{V_2}^2)^2} M^2 W_{\mu\nu}(x_1, Q_1^2) \mathcal{M}^{\mu\rho} \mathcal{M}^{\sigma\nu} W_{\rho\sigma}(x_2, Q_2^2) \frac{d^3 P_{X_1}}{(2\pi)^3 2E_{X_1}} \frac{d^3 P_{X_2}}{(2\pi)^3 2E_{X_2}} ds_1 ds_2 d\Gamma (2\pi)^4 \delta^4(P_1 + P_2 - P_{X_1} - P_{X_2} - P_{VV}) \quad (2)$$

where $g_W = g, g_Z = g/\cos\theta_W$, S is the square of the total machine energy, $s_i = (P_i + q_i)^2$ is the squared invariant mass of the remnant of proton i , and $d\Gamma$ is the vector-boson-scattering phase space.

At lowest order, no color is exchanged between the protons, and the remnants of the protons are color singlets. It follows that no QCD corrections due to gluon exchange between the first proton (or its remnant) and the second proton (or its remnant), or between either proton (or their remnants) and the products of the vector-boson-scattering subprocess, occur at $\mathcal{O}(\alpha_s)$. Therefore, the $\mathcal{O}(\alpha_s)$ correction to vector-boson scattering may be factorized into the corrections to the structure functions and the corrections to the vector-boson-scattering subprocess. This factorization is no longer true at $\mathcal{O}(\alpha_s^2)$, however. The structure functions are given at next-to-leading order in QCD by [5],

$$\begin{aligned} F_1(x, Q^2) &= \sum_i \left(C_{V_i}^2 + C_{A_i}^2 \right) \left\{ \int_x^1 \frac{dy}{y} \left[q_i(y, Q^2) + \bar{q}_i(y, Q^2) \right] \right. \\ &\quad \left. \left[\delta(1-z) - \frac{4}{3} \frac{\alpha_s(Q^2)}{\pi} z \right] - 2 \frac{\alpha_s(Q^2)}{\pi} \int_x^1 \frac{dy}{y} g(y, Q^2) z(1-z) \right\} \\ F_2(x, Q^2) &= 2x \sum_i \left(C_{V_i}^2 + C_{A_i}^2 \right) \left[q_i(x, Q^2) + \bar{q}_i(x, Q^2) \right] \\ F_3(x, Q^2) &= 4 \sum_i C_{V_i} C_{A_i} \left\{ \int_x^1 \frac{dy}{y} \left[-q_i(y, Q^2) + \bar{q}_i(y, Q^2) \right] \right. \\ &\quad \left. \left[\delta(1-z) - \frac{2}{3} \frac{\alpha_s(Q^2)}{\pi} (1+z) \right] \right\} \end{aligned} \quad (3)$$

where $z = x/y$, the sum runs over the flavors of all quarks and antiquarks which contribute to a given structure function, $C_{V_i} = C_{A_i} = 1/\sqrt{2}$ for W^\pm , and $C_{V_i} = T_{L_i}^3 - 2e_i \sin^2 \theta_W$, $C_{A_i} = T_{L_i}^3 = \pm \frac{1}{2}$ for Z . These expressions correspond to the DIS factorization scheme. The corresponding expressions in the $\overline{\text{MS}}$ scheme are obtained by replacing the quark and antiquark distribution functions in the leading-order terms by [6]

$$\begin{aligned}
q_i(x, Q^2) &= q_i^{\overline{\text{MS}}}(x, Q^2) \\
&+ \frac{1}{4} \frac{\alpha_s(Q^2)}{\pi} \int_x^1 \frac{dy}{y} g(y, Q^2) \left[[z^2 + (1-z)^2] \ln \left(\frac{1-z}{z} \right) + 8z(1-z) - 1 \right] \\
&+ \frac{2}{3} \frac{\alpha_s(Q^2)}{\pi} \int_x^1 \frac{dy}{y} q_i(y, Q^2) \left[(1+z^2) \left(\frac{\ln(1-z)}{1-z} \right)_+ - \frac{3}{2} \frac{1}{(1-z)_+} \right. \\
&\left. - \frac{1+z^2}{1-z} \ln z + 3 + 2z - \left(\frac{9}{2} + \frac{\pi^2}{3} \right) \delta(1-z) \right] \tag{4}
\end{aligned}$$

where the “plus” prescription is defined as usual (see, e. g., Ref. [5]).

If the structure functions, over the relevant ranges of x and Q^2 , were available from deep-inelastic scattering, they could be used directly, bypassing the parton model altogether. The typical Q^2 in vector-boson-scattering processes is M_V^2 , which is within the reach of HERA, but only for $x \gtrsim 0.1$ [7]. The possibility of using the measured structure functions directly will thus be limited to very high invariant masses for the vector-boson-scattering subprocess, $M_{VV} \sim 0.1 \sqrt{S}$. LEP \times LHC would be able to reach down to $x \sim 0.01$ at this value of Q^2 [8].

The validity of this approach relies on the factorization of the cross section that is inherent in Fig. 1. In order for the factorization to hold, two criteria must be satisfied. First, there must be no significant interference, at the parton level, between diagrams in which a quark from one proton and a quark from the other proton scatter into the same final-state quark. Kinematic arguments suggest that this interference

is very small [9], and we have verified that this is true in the example below. Second, the vector-boson-subprocess final state must be produced only via this mechanism, or dominantly so, or not interfere with similar final states. Examples include Higgs-boson production [2, 3], heavy-fermion production [10], and terms of enhanced electroweak strength in longitudinal-vector-boson scattering [1, 11].

As an explicit example of this approach, we calculate Higgs-boson production via vector-boson fusion at the LHC/SSC. The differential cross section is given by Eq. (2), with

$$\begin{aligned}
M^2 W_{\mu\nu}(x_1, Q_1^2) \mathcal{M}^{\mu\rho} \mathcal{M}^{\nu\sigma} W_{\rho\sigma}(x_2, Q_2^2) &= g_V^2 M_V^2 \left\{ F_1(x_1, Q_1^2) F_1(x_2, Q_2^2) \left[2 + \frac{(q_1 \cdot q_2)^2}{q_1^2 q_2^2} \right] \right. \\
&+ \frac{F_1(x_1, Q_1^2) F_2(x_2, Q_2^2)}{P_2 \cdot q_2} \left[\frac{(P_2 \cdot q_2)^2}{q_2^2} - M^2 + \frac{1}{q_1^2} \left(P_2 \cdot q_1 - \frac{P_2 \cdot q_2}{q_2^2} q_1 \cdot q_2 \right)^2 \right] \\
&+ \frac{F_2(x_1, Q_1^2) F_1(x_2, Q_2^2)}{P_1 \cdot q_1} \left[\frac{(P_1 \cdot q_1)^2}{q_1^2} - M^2 + \frac{1}{q_2^2} \left(P_1 \cdot q_2 - \frac{P_1 \cdot q_1}{q_1^2} q_1 \cdot q_2 \right)^2 \right] \\
&+ \frac{F_2(x_1, Q_1^2) F_2(x_2, Q_2^2)}{P_1 \cdot q_1 P_2 \cdot q_2} \left(P_1 \cdot P_2 - \frac{P_1 \cdot q_1 P_2 \cdot q_1}{q_1^2} - \frac{P_2 \cdot q_2 P_1 \cdot q_2}{q_2^2} + \frac{P_1 \cdot q_1 P_2 \cdot q_2 q_1 \cdot q_2}{q_1^2 q_2^2} \right)^2 \\
&+ \left. \frac{F_3(x_1, Q_1^2) F_3(x_2, Q_2^2)}{2 P_1 \cdot q_1 P_2 \cdot q_2} \left(P_1 \cdot P_2 q_1 \cdot q_2 - P_1 \cdot q_2 P_2 \cdot q_1 \right) \right\}. \tag{5}
\end{aligned}$$

For W^+W^- fusion one must sum over the W^+ (and the W^-) being emitted from either proton.

We show in Fig. 2 the total cross section for Higgs-boson production at the LHC/SSC through $\mathcal{O}(\alpha_s)$, using the next-to-leading-order parton distribution functions of Ref. [12], set S1-DIS. Also shown are the leading-order cross sections, evaluated using the leading-order parton distribution functions of Ref. [12], which were fit to the same data as set S1-DIS. The next-to-leading-order cross section at the SSC is 12% larger at $m_H = 100$ GeV, and 6% larger at $m_H = 800$ GeV, than the leading-order cross section. The corresponding increase at the LHC is 8% and 6%. Most

of the increase is due to the parton distribution functions, not to the explicit $\mathcal{O}(\alpha_s)$ corrections to the structure functions, because the total cross section is dominated by F_2 , which receives no QCD correction in the DIS scheme. To the extent that the next-to-leading-order parton distribution functions provide a better fit to the available data, and a more reliable extrapolation to high Q^2 , the next-to-leading-order cross sections in Fig. 2 represent the best predictions possible at this time.

The structure-function approach to vector-boson scattering makes it clear that the relevant scale of the structure functions, and therefore of the parton distribution functions, is the Q^2 of the vector boson. Since the typical Q^2 is about M_V^2 , the use of this fixed scale is a good approximation. Since the parton model breaks down at low Q^2 , and the parton distribution functions are available only for $Q^2 > 4 \text{ GeV}^2$, we have not included the region $Q^2 < 4 \text{ GeV}^2$ in our calculation. We estimate that this region contributes only about $4 \text{ GeV}^2/M_V^2 \sim 10^{-3}$ of the total cross section.

A heavy Higgs boson decays predominantly to W - and Z -boson pairs. The principal background to this signal at the LHC/SSC is W^+W^- and ZZ production via quark-antiquark annihilation. The QCD correction to the ZZ invariant-mass distribution increases the leading-order prediction by about 25% near threshold, up to about 60% at 800 GeV (for a factorization scale $\mu^2 = M_{ZZ}^2$) [13]. The corresponding increase for W^+W^- is about 45% near threshold and about 75% at 800 GeV [14]. The absence of a comparable increase in the Higgs-boson production cross section therefore decreases the signal-to-background ratio.

In the standard Higgs model, the Higgs boson is also produced at the LHC/SSC from gluon fusion via a top-quark loop [15] with a comparable or larger cross section than from vector-boson fusion (for $m_t > 100 \text{ GeV}$, $m_H < 800 \text{ GeV}$). The QCD correction to this process is known only for a light ($m_H < 2m_t$) Higgs boson [16], and

increases the cross section by 50% at the SSC and 100% at the LHC (for $\mu^2 = m_H^2$). It would be desirable to observe Higgs-boson production via gluon fusion and vector-boson fusion separately, since the former involves the coupling of the Higgs boson to the top quark, while the latter does not.

If the invariant mass of the vector-boson-scattering subprocess is large compared to M_V , the cross section is dominated by the region $Q^2 \lesssim M_V^2$. One can then derive a distribution function for vector bosons carrying a fraction x of the proton's momentum [3, 17]. In terms of hadronic structure functions, we find

$$\begin{aligned}
 f_T(x) &= \frac{g_V^2}{32\pi^2} \frac{1}{x} \int_x^1 \frac{dy}{y} \left[F_2(y, M_V^2) \left(1 - \frac{x}{y}\right) + F_1(y, M_V^2) \frac{x^2}{y} \right] \ln \left(1 + \frac{Sy(y-x)}{M_V^2}\right) \\
 f_L(x) &= \frac{g_V^2}{32\pi^2} \frac{1}{x} \int_x^1 \frac{dy}{y} \left[F_2(y, M_V^2) \left(1 - \frac{x}{2y}\right)^2 - \frac{1}{2} F_1(y, M_V^2) \frac{x^2}{y} \right] \quad (6)
 \end{aligned}$$

where the subscripts T, L denote the polarization of the vector boson (the two transverse polarizations have been averaged). At leading order in QCD, $F_2(y, Q^2) = 2yF_1(y, Q^2)$ (Callan-Gross relation), and the expressions above reduce to the usual parton-model formulae. The $\mathcal{O}(\alpha_s)$ expressions for the vector-boson distribution functions are obtained simply by using the next-to-leading-order expressions for the structure functions, Eq. (3). It has already been shown that there are no terms of $\mathcal{O}(\alpha_s\pi)$ (from soft gluons) in the DIS scheme [18] (although there are in the $\overline{\text{MS}}$ scheme), as is evident from Eq. (3). In any case, the $\mathcal{O}(\alpha_s\pi)$ terms generally do not dominate at LHC/SSC energies.

Acknowledgements

We are grateful for conversations with S. Dawson, D. Dicus, K. Ellis, W. Giele, J. Morfin, C. Quigg, G. J. van Oldenborgh, and W.-K. Tung. T. H. was supported by an SSC Fellowship from the Texas National Research Laboratory Commission (TNRLC) under Award No. FCFY9116. S. W. was supported by an SSC Fellowship from the TNRLC and by contract number DE-AC02-76-CH-00016 with the U.S. Department of Energy.

References

- [1] M. Chanowitz and M. K. Gaillard, Nucl. Phys. **B261**, 379 (1985).
- [2] R. Cahn and S. Dawson, Phys. Lett. **136B**, 196 (1984).
- [3] G. Kane, W. Repko, and W. Rolnick, Phys. Lett. **148B**, 367 (1984).
- [4] M.-S. Chen, I. Muzinich, H. Terazawa, and T. Cheng, Phys. Rev. **D7**, 3485 (1973).
- [5] G. Altarelli, R. K. Ellis, and G. Martinelli, Nucl. Phys. **B143**, 521 (1978); **B146**, 544(E) (1978); **B157**, 461 (1979).
- [6] W. Bardeen, A. Buras, D. Duke, and T. Muta, Phys. Rev. **D18**, 3998 (1978).
- [7] J. Feltesse, in *Proceedings of the HERA Workshop*, Hamburg, 1987, ed. R. Peccei (DESY, 1988), p. 33.
- [8] J. Blümlein, J. Feltesse, and M. Klein, in *Proceedings of the ECFA Large Hadron Collider Workshop*, Aachen, edited by G. Jarlskog and D. Rein, CERN 90-10 (1990), p. 830.
- [9] D. Dicus and S. Willenbrock, Phys. Rev. **D32**, 1642 (1985).
- [10] O. Éboli et al., Phys. Rev. **D34**, 771 (1986); Phys. Lett. **178B**, 77 (1986); S. Dawson and S. Willenbrock, Nucl. Phys. **B284**, 449 (1987).
- [11] Z. Kunszt and D. Soper, Nucl. Phys. **B296**, 253 (1988).
- [12] J. Morfin and W.-K. Tung, Z. Phys. **C52**, 13 (1991).
- [13] J. Ohnemus and J. Owens, Phys. Rev. **D43**, 3626 (1991); B. Mele, P. Nason, and G. Ridolfi, Nucl. Phys. **B357**, 409 (1991).

- [14] J. Ohnemus, Phys. Rev. **D44**, 1403 (1991).
- [15] H. Georgi, S. Glashow, M. Machacek, and D. Nanopoulos, Phys. Rev. Lett. **40**, 692 (1978).
- [16] S. Dawson, Nucl. Phys. **B359**, 283 (1991); A. Djouadi, M. Spira, and P. Zerwas, Phys. Lett. **264B**, 440 (1991).
- [17] M. Chanowitz and M. K. Gaillard, Phys. Lett. **142B**, 85 (1984); S. Dawson, Nucl. Phys. **B249**, 42 (1985).
- [18] S. Dawson, Phys. Lett. **217B**, 347 (1989).

Figure Captions

- Fig. 1: Structure-function approach to vector-boson scattering in pp collisions.
- Fig. 2: Total cross section for Higgs-boson production via vector-boson fusion at the (a) LHC and (b) SSC, versus the Higgs-boson mass. The solid curves are calculated at next-to-leading order in QCD, using set S1-DIS of Ref. [12]. The dashed curves are calculated at leading order, using the leading-order set of Ref. [12]. The cross sections due to an intermediate W^+W^- and ZZ pair are shown separately.

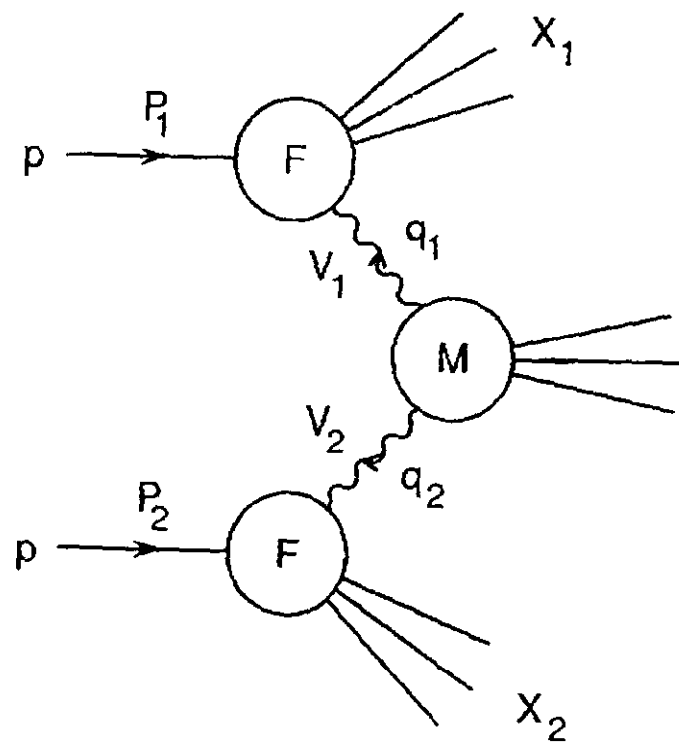


Fig. 1

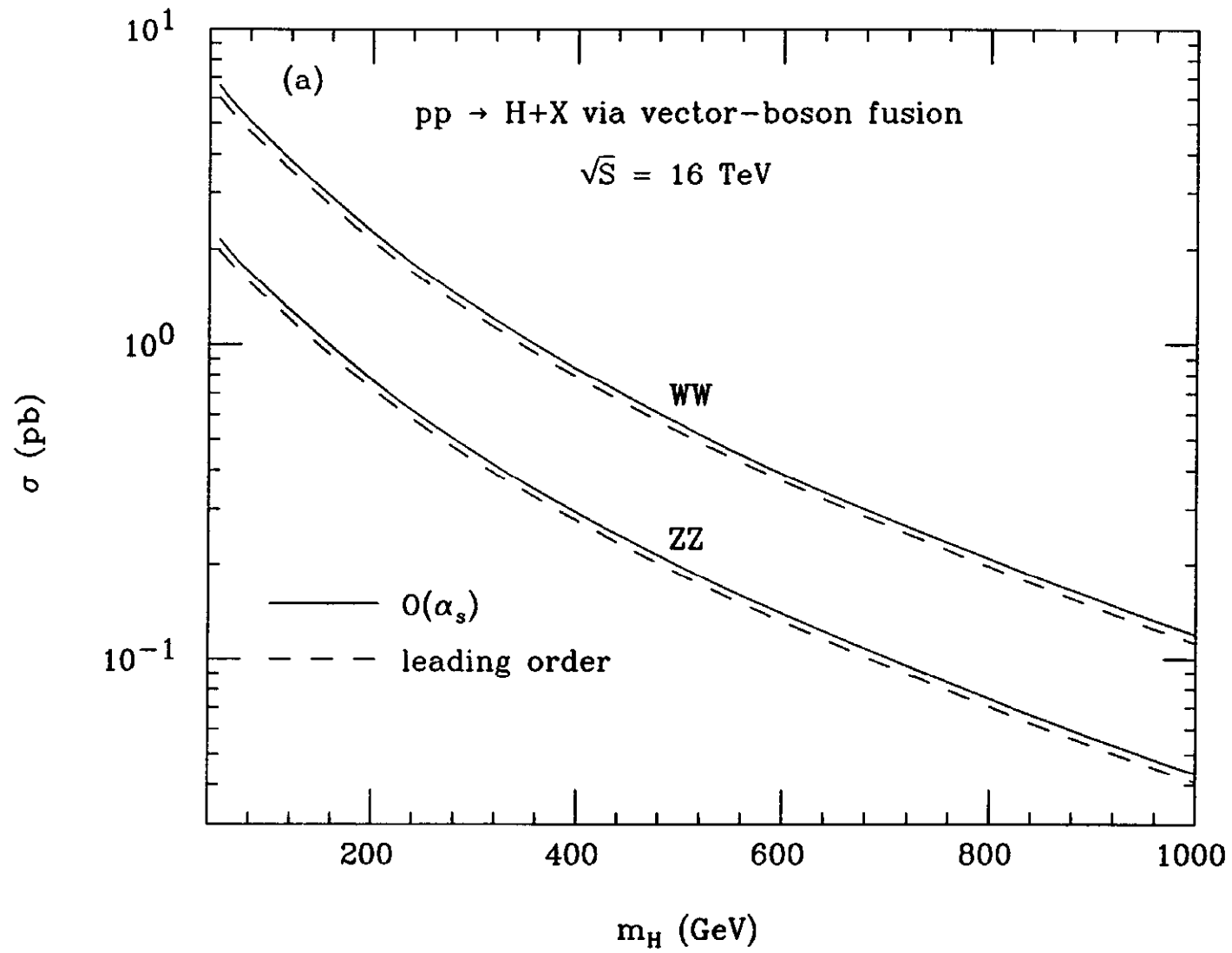


Fig. 2

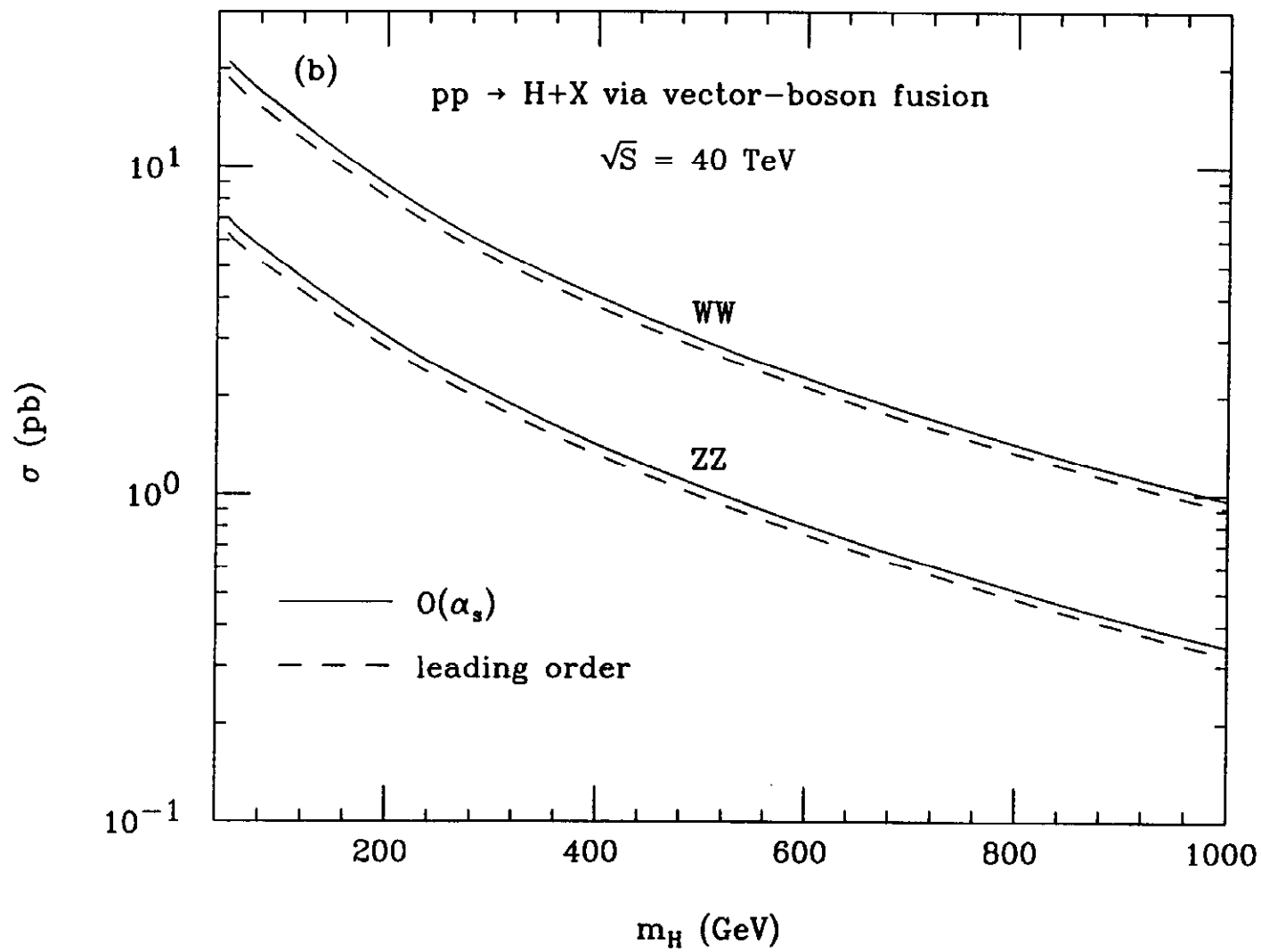


Fig. 2